Contrib. Astron. Obs. Skalnaté Pleso **38**, 5 – 11, (2008)

Latitude-time distribution of the solar magnetic fields from 1975 to 2006

M. Minarovjech

Astronomical Institute of the Slovak Academy of Sciences
059 60 Tatranská Lomnica, The Slovak Republic, (E-mail: milanmin@ta3.sk)

Received: April 26, 2007; Accepted: August 31, 2007

Abstract. This paper presents the solar magnetic field distribution and meridional migration for the period of 1975-2006. A magnetic field latitude-time distribution map covering a 32-year period has been investigated. For this purpose a modified latitude-time diagram of the solar magnetic field distribution containing different kinds of fine structures is used.

Key words: sun – magnetic fields – solar cycle

1. Introduction

Turbulent fluid motions interacting with the ionized gas within the Sun, and within its atmosphere, are believed to feed electrical currents flowing in the solar plasma and generate magnetic fields. The tremendous progress in the solar magnetic fields research was activated by the creation of the magnetograph (Babcock, Babcock 1955). The evolution of the large-scale solar magnetic fields in the course of solar cycle is accompanied by the global patterns represented by 'butterfly' diagram as plots of mean radial magnetic fields versus heliocentric latitude and time.

The magnetic fields variable in their polarity and magnitude migrate on the solar surface from the activity belts poleward during the course of a solar cycle (e.g. Bumba, Howard 1965; Wang *et al.*, 1989; Obridko *et al.*, 2006). The migration and reversals of the polar magnetic fields were initially observed using magnetograph data. Because most of the structures in the solar atmosphere are related to the solar magnetic fields, a possible way to follow the evolution of large-scale magnetic field patterns is by plotting tracers of the magnetic field such as quiescent filaments, polar faculae, or the coronal green line (Leroy, Noens 1983; Makarov, Sivaraman 1989; Callebaut, Makarov 1992; McIntosh 1992; Makarov *et al.* 2001; Minarovjech *et al.* 2007). The purpose of this paper is to determine the solar magnetic field distribution over the solar surface and time directly from measurements of the solar magnetic fields.

2. Data

The data used for this study comprise three data sets. The first one is the data set of all available NSO/Kitt Peak synoptic magnetogram maps (`URL: ftp://nsokp.nso.edu/kpvt/synoptic/mag/`) in the form of 180 by 360 arrays beginning at Carrington rotation (CR) number 1625, starting at year 1975.13, through CR 2006, ending at 2003.66. The data for missing CR 1640 to CR 1644 and CR 1854 were filled in by interpolation. The second one, SOHO/MDI magnetic field synoptic charts (`URL: http://soi.stanford.edu/magnetic/index6.html`) beginning at CR 1909 starting at year 1996.34, until CR 2051, ending at 2007.02. All SOHO/MDI synoptic magnetogram maps were interpolated into 180 by 360 data arrays. The third one, net (signed) flux frames of magnetic synoptic FITS files obtained by the Vector Spectromagnetograph (VSM), a part of NSOs Synoptic Optical Long-term Investigations of the Sun (SOLIS) instrumental package (`URL: ftp://solarch.tuc.noao.edu/synoptic/level3/vsm/merged/carr-rot/`) beginning at CR 2007 until CR 2051.

The all kinds of synoptic magnetogram maps are represented now as i-by-j data arrays containing net magnetic flux data $\phi_{i,j,n}$ for each n-th CR file, where $1 \geq i \geq 180$ and $1 \geq j \geq 360$. The array rows are equal increments of the sine of the solar latitude and the columns are increments of the Carrington longitude and array data. The used period for CR 1625 to 2051 thus reaches $n = 427$ CR.

For all arrays we take longitudinally averaged values. This gives the one-dimensional data 1 by 180 stripes. The i-th element of n-th stripe contains the corresponding averaged net magnetic flux $\phi_{S_{i,n}}$ expressed by equation (1)

$$\phi_{S_{i,n}} = \frac{\sum_{j=1}^{360} \phi_{i,j,n}}{360}. \tag{1}$$

The resulting averages of both KPVT and SOHO/MDI synoptic magnetogram maps for CR 1909 until CR 2006 are used to rescale and merge the SOHO/MDI data stripes for CR 2007, starting at year 2003.66 to CR 2051 and the NSO/Kitt Peak data stripes by using the least squares method. Because the current SOLIS-VSM FITS data products are preliminary, the rescaled SOHO/MDI data were used and the same method was applied to rescale the VSM data. The resulting KPVT and VSM stripes were inserted into a two-dimensional 427 by 180 magnetic flux matrix. The elements of the magnetic flux matrix represent longitudinally averaged and re-scaled values of the line-of-sight magnetic flux, or net 'averaged magnetic flux' (AMF).

The latitudes in the original synoptic magnetogram maps are represented as the sine of heliographic latitude. In order to better demonstrate the higher latitudes, the sine latitude scale is converted to the linear latitude scale.

Figure 1 shows the usual latitude-time distribution of the AMF from magnetic field matrix, analogous to the well-known Maunder butterfly diagram for sunspots. Bright/dark gray color denotes the positive/negative polarity. The magnetic flux scale coding is shown in colorbar (Fig. 1 right panel). As it can be seen, the equatorward drifts of the active latitudes and some poleward meridional flows, both with polarity reversal at the poles every 11 years are evident.

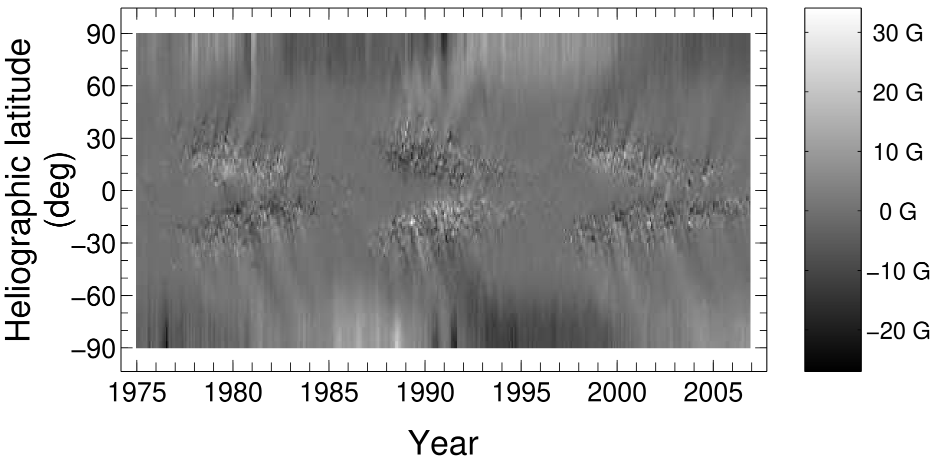

Figure 1. A latitude-time distribution of the AMF. Note the linear latitude axis.

Figure 2 shows the total (unsigned) AMF, obtained by using the same method as above, except that the absolute value of the flux $\phi_{i,j,n}$ was calculated before doing the average over longitude for each Carrington rotation. The i-th element of n-th stripe contains now a corresponding averaged total magnetic flux $\phi_{S_{i,n}}$ expressed by equation (2)

$$\phi_{S_{i,n}} = \frac{\sum_{j=1}^{360} \mid \phi_{i,j,n} \mid}{360}. \tag{2}$$

For better contrast, a logarithmic scale to the AMF intensity is applied

$$AMF_D = log(abs(AMF) + 1) \tag{3}$$

and the AMF_D values are displayed.

3. Data processing

It is known that the magnetic fields on the Sun play a dominant role in almost all processes in the solar atmosphere. For many solar activity phenomena (e.g. sunspots, prominences) its manifestation is independent of the polarity of magnetic field. To study the latitude-time distribution of the magnetic fields independently of arrangement of the polarity, an alternative processing method

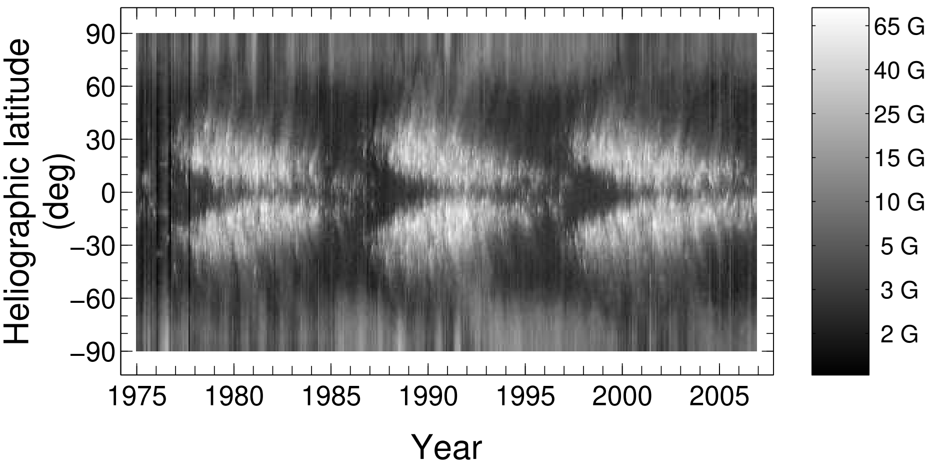

Figure 2. A latitude-time distribution of the total AMF. Note the logarithmic scale for the magnetic flux.

is described below. The data in the magnetic field matrix were converted to their absolute values. Data for missing CR 1640 to CR 1644, obtained by interpolation, have been replaced by constant values of 5 in order to prevent the formation of artificial patterns. The i-th element of n-th stripe contains in this case an averaged net magnetic flux $\phi_{S_{i,n}}$ expressed by equation (4)

$$\phi_{S_{i,n}} = \frac{\mid \sum_{j=1}^{360} \phi_{i,j,n} \mid}{360}. \tag{4}$$

To better represent the converted AMF matrix, a logarithmic scale to the AMF intensity is applied as it can be seen in Figure 3.

The resulting patterns shown in Fig. 3 yield a modified, alternative representation of the complex AMF latitude-time distribution and migration in the course of the solar cycle. The gray scale coding for the absolute values of AMF intensity is shown in colorbar (Fig. 3 right panel). In Fig. 3 we can clearly distinguish many well-defined AMF patterns. Note that the interpolated data for missing CR 1640 to CR 1644 (year 1976), depicted as a dark vertical strip, and dark notches in the vicinity of the poles in the period of 2003-2006 are only artificial structures. The high latitudes are characterized by the single or multiple poleward drifting dark AMF low intensity belts which represent the boundary between opposite polarity of the high latitude magnetic fields. The slow equatorward migration of the magnetic activity patterns, co-spatial with the sunspot formation belts is clearly differentiable as the spotted dark and bright zonal patterns located in the mid- and low- latitudes. Poleward moving streams connected to the high-latitude magnetic fields are beginning to occur

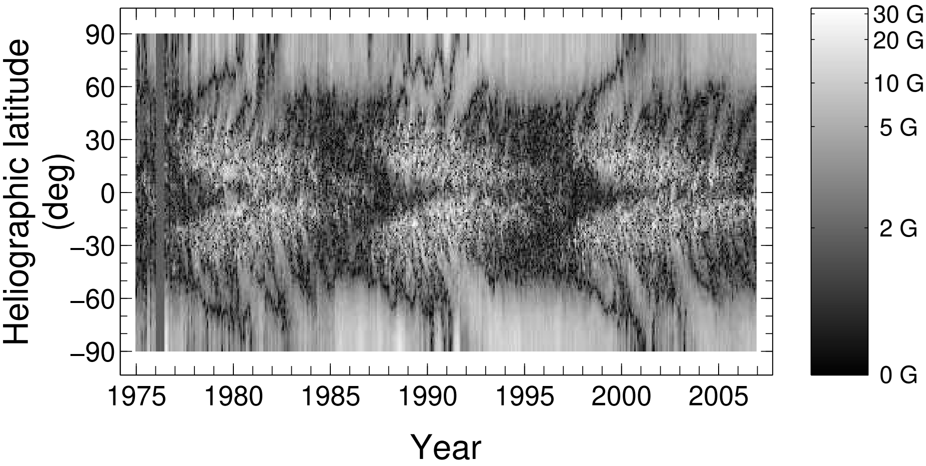

Figure 3. A latitude-time plot of the AMF in the absolute values. See the text for details. Note a logarithmic intensity scale and linear latitude axis

in the magnetic activity patterns as it can be seen in Fig.3 through most of the cycle.

The weak AMF fields are discernible as dark areas at mid and low latitudes. Distribution and migration of the last AMF fields in the course of the solar cycle is complex. The low-latitude boundary parts of this pattern are drifting equatorward. As the evolution of solar cycle approaches the minimum, the mid-latitude parts of this pattern are separated into the high latitude poleward migrating belts and low-latitude equatorward migrating parts. The both parts then disappear around the time of the next solar cycle maximum.

The structure of the AMF latitude-time distribution is complex. However, we should categorize the shown AMF structures into three different sections, recurring cyclically approximately every 11 years by using their patterns composition and boundary. To the first section belong the AMF activity patterns, appearing in the latitudes around 30° and migrating equatorward with the progress of the solar cycle. The second section incorporates the low- and mid- latitude AMF regions characterized by the complex distribution and low AMF flux located in the latitude ranges 0°- 50° depending on the phase of solar cycle. The third section seems to denote polar- and high-latitude regions (latitudes above 50°) outlined on the time axis by the primary poleward migrating boundary zones between the opposite polarities of the high-latitude magnetic fields.

4. Discussion and conclusions

This paper presents an alternative view to the longitudinally averaged standard synoptic magnetogram maps with the intent to determine the latitude-time distribution of magnetic fields, represented by the absolute values of the AMF, during the period of 1975-2006. No attempt was made to apply any additonal correction to the Sun's axial tilt.

In Fig. 3 one can identify at least three in each solar cycle recurring sections of the AMF patterns characterized by a different kind of the AMF distribution and different directions of migration of their sector boundaries. The details of AMF patterns are individual for the northern and southern hemisphere, and for each solar cycle. We note the non-monotonous poleward migration of the AMF boundaries between opposite magnetic polarities, probably caused by changes in the mid- and higher- latitude magnetic field activity during solar cycle 22. We are unable to generalize the course of the individual AMF poleward migrate structures, however, it seems that the complexity of their course is directly proportional to the strength of solar cycle.

Here it is interesting to note that in Fig. 3 there is no indication of the migration trajectories of "magnetic neutral lines" (alias filament bands) of the large-scale magnetic fields derived from H_α synoptic charts by Makarov *et al.* (2001) for the latitude range $\pm 30°$. On the other hand, the migration trajectories in the latitudes above 30° correspon to the boundaries between the AMF sectors 2 and 3 including the primary poleward migrating boundary zones between the opposite magnetic polarities of the high-latitude magnetic fields.

It is clear in Fig. 3 that we are able now to estimate the individual high-latitude poleward drift speed and course of the AMF boundary between the opposite magnetic field polarity, after the boundary splitting at 45°, in a more precise and detailed way. Since mid- 50's the solar dynamo theories are developed for modelling the solar cycle. In this paper we propose the modified alternative view to large-scale solar cycle features of the AMF, which then may provide some novel insights into the behaviour of the solar dynamo, as well as into the large-scale latitude-time distribution of the solar activity phenomena (e.g., solar corona and prominences).

5. Acknowledgement

SOLIS data used here are produced by support from NSF and NASA. The National Solar Observatory is operated by AURA, Inc. under a cooperative agreement with the National Science Foundation. This paper was supported by the Grant Agency VEGA of the Slovak Academy of Sciences, under Contract 2/7012/27 and by the Science and Technology Assistance Agency APVT under Contract No. APVT 51-012-704. The author thanks the anonymous referee for constructive comments and suggestions.

References

Babcock, H.W., Babcock, H.D.: 1955, *Astrophys. J.* **121**, 349

Bumba, V., Howard, R.: 1965, *Astrophys. J.* **141**, 1502

Callebaut, D.K., Makarov, V.I.: 1992, *Sol. Phys.* **141**, 381

Leroy, J.L., Noens, J.C.: 1983, *Astron. Astrophys.* **120**, 1L

Makarov, V.I., Sivaraman, K.R.: 1989, *Sol. Phys.* **119**, 35

Makarov, V.I., Tlatov, A.G., Sivaraman, K.R.: 2001, *Sol. Phys.* **202**, 11

McIntosh, P.S.: 1992, in *The Solar Cycle*, ed.: K.L. Harvey, ASP Conf. Ser., **27**, 14

Minarovjech, M., Rušin, V., Saniga, M.: 2007, *Sol. Phys.* **241**, 263

Obridko, V.N., Sokoloff, D.D. Kuzanyan, K.M. Shelting, B.D., Zakharov, V.G.: 2006, *Mon. Not. R. Astron. Soc.* **365**, 827

Wang, Y.M., Nash, A.G., Sheeley N.R.: 1989, *Astrophys. J.* **347**, 529